Int. J. Heat Mass Transfer. Vol. 27, No. 11, pp. 2015–2023, 1984
Printed in Great Britain

0017 9310/84 $3.00 + 0.00
Pergamon Press Ltd.

Heat transfer phenomena in liquid–liquid spray columns

H. NOTH and A. MERSMANN

Lehrstuhl B für Verfahrenstechnik, Technische Universität München,
Arcisstraße 21, 8000 München 2, Federal Republic of Germany

(*Received* 3 *June* 1983 *and in revised form* 15 *September* 1983)

Abstract—Heat transfer experiments were carried out concerning the transfer from cylindrical surfaces immersed in liquid–liquid spray columns 100 and 200 mm in diameter. Water, formamide, glycerol, tetrachloroethylene, tetrabromoethane, toluene and 2-ethylhexanol were used to study the influence of physical properties of immiscible liquids over a wide range. Operating conditions (liquid flow rate of the dispersed phase, equipment geometry) affect the heat transfer comparatively to a low degree. Physical properties of the heating surface were varied to examine the influence of wetting phenomena on the heat transfer coefficient. The calculation model presented in this paper is based on equations of the heat transfer in a single phase flow over a flat plate. Heat transfer is described by Reynolds number incorporating the relative velocity between the drops and the continuous phase, the equivalent diameter and the viscosity of the continuous phase.

INTRODUCTION

LIQUID–LIQUID spray columns are used in the field of reaction engineering and extraction. Many liquid–liquid processes require heat transfer between dispersed systems and cooling or heating surfaces. Till now there have been no investigations about the heat transfer between heat exchanger walls and dispersed liquid–liquid systems in spray columns. In such contactors liquid drops are dispersed into another continuous immiscible liquid. These drops, 1–10 mm in diameter, either rise or fall depending on mass densities. The heat transfer process between the transfer surface and the liquid–liquid dispersion is described by the heat transfer coefficient α as a function of the superficial velocity $\dot{v}_d$ of the dispersed phase. The heat transfer coefficient α is defined as

$$\alpha = \frac{\Phi}{A(\theta_w - \theta_b)} \tag{1}$$

is determined by measuring the heat flux which is transferred between the liquid–liquid systems and the heat exchanger, divided by the heat transfer area A and the temperature difference $\theta_w - \theta_b$. Figure 1 shows a typical measured curve of the heat transfer coefficient vs the superficial velocity $\dot{v}_d$ of the dispersed phase. The curve ends at the flooding point. The superficial velocity of the flooding point is reached when the dispersed phase begins to displace the continuous phase to the top of the column. Figure 1 also shows the heat transfer of a single phase water flow. The high rates of the two-phase heat transfer coefficients in comparison with the results of a single phase flow, are caused by the intensive mixing of the continuous phase. This is induced by the motion of the rising drops. Wetting phenomena on the heat transfer surface have a strong effect on the heat transfer coefficients. At the end of this paper a calculation method is given for the special case that the heat transfer surface is completely wetted by a thin film of the dispersed phase.

EXPERIMENTAL SET-UP

Two spray columns 100 and 200 mm in diameter were used to determine heat transfer coefficients, see Fig. 2(a). Drops of the dispersed phase were formed at a sieve plate mounted at the bottom of the column. They rose due to their buoyancy forces. The heat transfer probe was axially adjustable and immersed in the liquid–liquid dispersion. The bulk temperature was measured by thermocouples at several points. A cross-section of the heat transfer probe is shown in Fig. 2(b). An electrical heating coil was enclosed by a cylindrical shell made of copper. The surface temperature of the probe was measured by thermocouples soldered on the surface. Thin-walled sleeves of chrome–nickel steel attached to both ends of the heat transfer part of the probe reduced axial heat loss to a minimum.

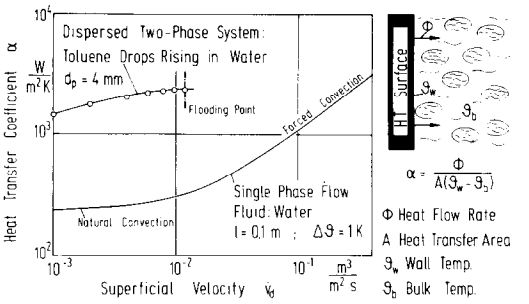

FIG. 1. Heat transfer function measured in a dispersed liquid–liquid system (toluene dispersed in water) in comparison with experimental results of heat transfer on a flat plate.

NOMENCLATURE

A	heat transfer area
A_h	cross-sectional area of the heater
a	thermal diffusivity
c, c_p	specific heat capacity
D^*	equivalent diameter
d_H	diameter of the heater
d_h	hydraulic diameter
d_p	drop diameter
g	gravitational acceleration
h	distance between drops
L_F	length of the film
L_H	length of the heat transfer area
l	characteristic length
$\dot{m}_d$	mass flow rate of the film
s	thickness of the film
u	perimeter of the heater
$\dot{V}_d$	flow rate of the film
$\dot{v}_d$	superficial velocity
w	velocity
w_s	terminal velocity
w_{ss}	velocity of drops in a swarm
w_{rel}	relative velocity between the phases
w_E	terminal velocity of a fluid particle with maximum stable size.

Greek symbols

α	heat transfer coefficient
α_d	heat transfer coefficient of the film
$\alpha_{d,dis}$	heat transfer coefficient between film and liquid–liquid dispersion
α_{tot}	total heat transfer coefficient
ε	volume fraction
η	dynamic viscosity
θ	temperature
λ	thermal conductivity
ν	kinematic viscosity
ρ	density
$\Delta\rho$	density difference
$\gamma_{1,2}$	surface or interfacial tension
ϕ	heat flow rate.

Subscripts

b	bulk
c	continuous
d	dispersed
l	characteristic length
max	maximum
w	wall.

Dimensionless numbers

Nu	$\alpha D^*/\lambda_c$
Nu_d	$\alpha_d s/\lambda_d$
Re	$\dot{v}_d D^*/\varepsilon_d \nu_c$
Re_d	$\dot{V}\rho_d/\eta_d u$
Pr	ν/a.

Heat transfer coefficients were measured in several liquid–liquid systems at various superficial velocities $\dot{v}_d$ of the dispersed phase, see Table 1.

Table 2 shows the wide range of liquid properties. To avoid corrections owing to the temperature dependence of the liquid properties the temperature differences $\Delta\theta$ were chosen only in the range 1–3 K.

Heat transfer measurements were carried out with probes of different lengths of effective heat transfer area. Results of these investigations are shown in Fig. 3. Using probes with a length $L_H > 100$ mm the measured data can be used as data representative for long heating or cooling pipes which are installed in liquid–liquid spray columns.

Certain wetting conditions at the heater surface were realized by several treatments. Metallic probes plated with copper show hydrophilic behaviour. On the other hand hydrophobic properties were achieved by coating with PTFE or modified PTFE (FEP).

EXPERIMENTAL RESULTS

The shape and the maximum value of a curve of the heat transfer coefficient vs superficial velocity of a

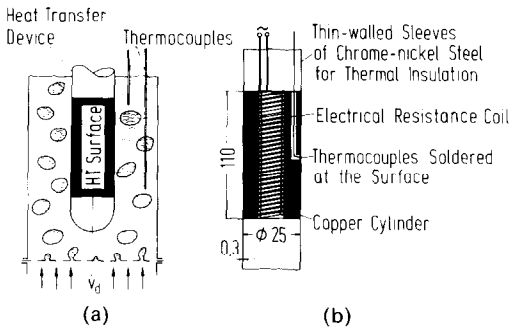

FIG. 2. (a) Arrangement for measurement of heat transfer. (b) Cross-section of the heat transfer probe.

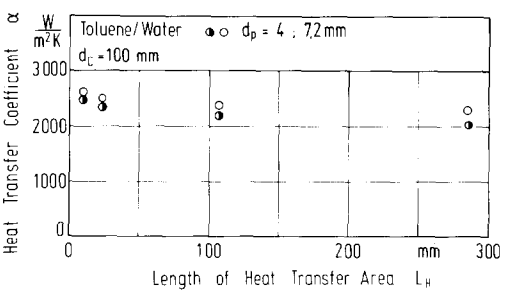

FIG. 3. The effect of heater length on the heat transfer from vertical heating probes toluene–water, $\dot{v}_d = 4 \times 10^{-3}$ m s^{-1}.

Table 1. Liquid–liquid systems range of superficial velocity $0.001 < \dot{v}_d < 0.02$ m s^{-1}

Dispersed phase	Continuous phase	Drop diameter (mm)	Interfacial tension (10^3 N m^{-1})
2-Ethylhexanol	Water	2.6–3.7	16
Toluene	Water	2.7–10	36
Toluene	Formamide	2.8–5.2	25
Toluene	Aqueous glycerol (60%)	3.7–6	28
Toluene	Aqueous glycerol (69%)	3.6–5.9	28
Water	Tetrachloroethylene	2.5–5.5	41
Water	Tetrabromoethane	2.2–3.1	39

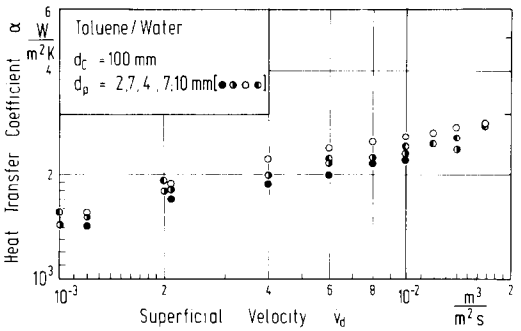

FIG. 4. Variation of heat transfer coefficient with superficial velocity. Parameter: drop diameter, toluene–water.

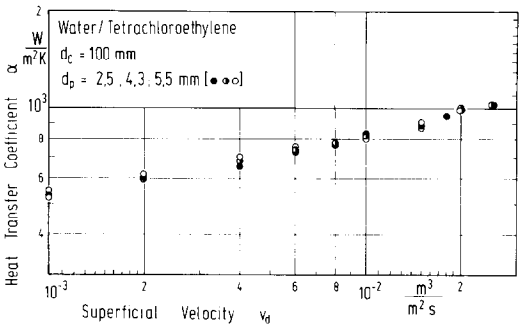

FIG. 5. Variation of heat transfer coefficient with superficial velocity. Parameter: drop diameter, water–tetrachloroethylene.

liquid–liquid system depends on wetting phenomena of the heat transferring surface. In the following section it is assumed that the heat transfer surfaces are completely covered with the continuous phase. Figure 4 shows heat transfer curves $\alpha = f(\dot{v}_d)$ of various toluene–water systems. As the drop diameter increases the heat transfer improves. The highest values were obtained with 7 mm toluene drops. The heat transfer coefficients rise from 1650 up to 2750 W m^{-2} K^{-1} at the flooding point. The average slope of the heat transfer function is 0.2. Measurements of rising toluene drops in water have shown that 7 mm drops rise with the highest velocity.

Experimental heat transfer results of a water–tetrachloroethylene column are shown in Fig. 5. The scattering of the heat transfer coefficients with the drop diameter is small and is caused by the limited accuracy of the measuring technique. Water drops in tetrachloroethylene with diameters of 2.5, 4.3 and 5.5 mm have the same terminal velocities. The heat transfer of the water–tetrachloroethylene system is only 1/3 of the value of the toluene–water system.

Similar data were obtained with the water–tetrabromoethane system, see Fig. 6. As a result of the low thermal conductivity λ_c and the high viscosity ν_c of the tetrabromoethane used as the continuous phase, the maximum of the heat transfer coefficient is reached at only 480 W m^{-2} K^{-1}. Experimental data of the 2-ethylhexanol–water system show again a small

Table 2. Physical properties of liquids

	Mass density ρ (kg m^{-3})	Kinematic viscosity ν (10^{-6} m^2 s^{-1})	Thermal conductivity λ (10^{-3} W m^{-1} K^{-1})	Specific heat capacity c_p (J kg^{-1} K^{-1})	Prandtl number Pr
Water	998	1	604	4182	7
Toluene	867	0.67	141	1717	7
2-Ethylhexanol	833	11	160	2345	134
Tetrachloroethylene	1621	0.56	158	897	5
Tetrabromoethane	2960	3.9	89	400	52
Formamide	1134	3.2	350	2382	25
Glycerol (60%)	1156	9	390	3760	100
Glycerol (69%)	1180	16	360	3635	190

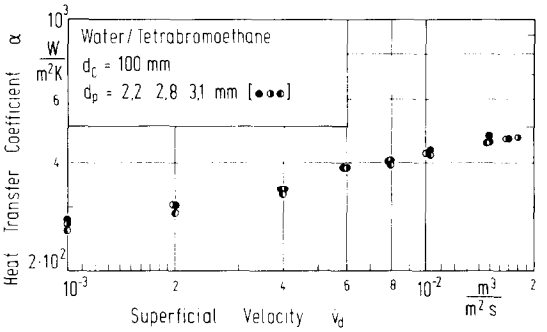

FIG. 6. Variation of heat transfer coefficient with superficial velocity. Parameter: drop diameter, water–tetrabromoethane.

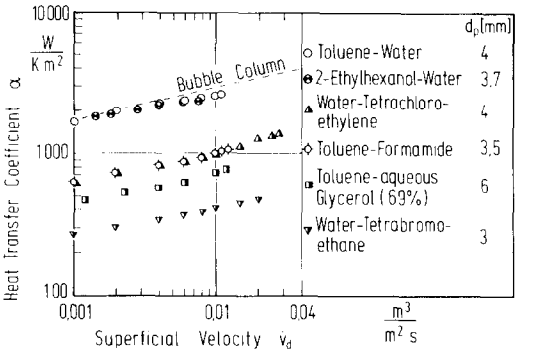

FIG. 8. Variation of the heat transfer coefficient with the superficial velocity of all liquid–liquid systems used in this paper (each liquid–liquid system is presented by only one measurement series with a certain drop diameter).

influence on the drop diameter, see Fig. 7. The heat transfer function corresponds well with the toluene–water results.

Information about the effect of the physical properties of the liquid is given in Fig. 8. Each liquid–liquid system investigated is represented by data valid for a certain drop diameter. Regarding the great number of possible influencing physical properties ρ_c, ρ_d, η_c, η_d, λ_c, λ_d, c_c, c_d, $\gamma_{1,2}$ only some remarks are given here about the most important parameters. The highest heat transfer rates were obtained in the toluene–water and 2-ethylhexanol–water systems. Obviously these results originate from the high thermal conductivity and high specific heat capacity of the water. Investigations of the heat transfer in bubble columns [1, 2] and gas fluidized beds [3, 4] have shown that the main temperature drop in the surrounding of the heat transfer surface takes place in a layer whose thickness is frequently smaller than the particle diameter. Very close to the heating or cooling surface a layer exists which mainly contains a continuous phase. Assuming similar conditions on the heat transfer surface in a liquid–liquid spray column the heat transfer therefore is governed by the physical properties and the fluid dynamics occurring in the thin layer near the wall. Consequently the lowest heat transfer coefficients were obtained in the water–tetrabromoethane system,

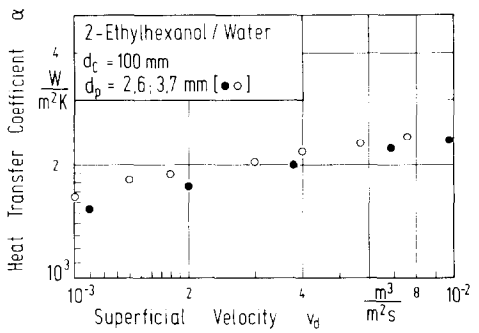

FIG. 7. Effect of the superficial velocity and the drop diameter on the heat transfer coefficient in the 2-ethylhexanol–water system; rising velocity of the 2.6 mm drops $w_s = 0.1\ m\ s^{-1}$ and of the 3.7 mm drops $w_s = 0.12\ m\ s^{-1}$.

which has a high viscosity ν_c and low thermal properties λ_c, c_c of the continuous phase. Since convective heat transfer is always influenced by fluid dynamics this phenomenon must be considered. When a liquid is dispersed into a continuum of another immiscible liquid a swarm of drops rises or falls depending on the mass densities of the two liquids. If the density difference between the two liquids and the viscosity of the continuous phase is not too large, the liquid–liquid spray column will have a homogeneous structure. This means that the velocity of the drops and the volume fraction of both liquids are equal in the whole column. In contrast gas fluidized beds and bubble columns usually have a heterogeneous structure. A part of the fluidized gas rises through the bed in the form of large bubbles or bubble agglomerates. In many cases the velocity of these bubbles is considerably higher than the superficial velocity of the gas. In a homogeneous liquid–liquid system the volume fraction ε_d of the dispersed phase increases with the superficial velocity $\dot{v}_d$. The swarm velocity, i.e. the rising velocity of drops in a swarm, is identical with the average relative velocity w_{rel} between the drops and the continuous phase. Rearranging the equation of continuity, the relative velocity w_{rel} can be written as the ratio of the superficial velocity $\dot{v}_d$ and the volume fraction ε_d

$$w_{rel} = \frac{\dot{v}_d}{\varepsilon_d}. \tag{2}$$

The relative velocity characterizing the fluid dynamics in homogeneous spray columns can be calculated by using an expansion diagram as shown in Fig. 9. The volume fraction ε_d is plotted vs the ratio $\dot{v}_d/w_s$. Experimental data of several liquid–liquid systems are correlated by equation (3)

$$\frac{\dot{v}_d}{w_s} = \varepsilon_d \cdot \varepsilon_c^2. \tag{3}$$

The terminal velocity w_s of single drops rising in an immiscible liquid can be calculated by different procedures [5, 6].

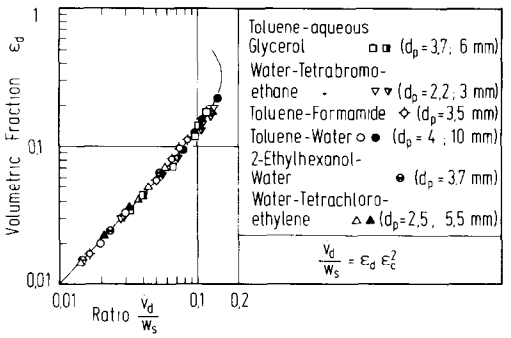

FIG. 9. Volume fraction vs v_d/w_s ratio (w_s is the terminal velocity of a single drop in an infinite medium).

EXISTING CALCULATION METHOD

As mentioned above there are no methodical investigations about the heat transfer between heating or cooling surfaces and dispersed liquid–liquid systems. In connection with a comprehensive investigation about the heat transfer from solid heat transfer surfaces to dispersed two-phase systems Mersmann [7] presented some experimental data obtained in toluene–water and water–tetrachloroethylene systems. He established a calculation method for the maximum heat transfer in dispersed systems based on a diagram containing the controlling dimensionless groups of heat transfer. The Nusselt number formed with the particle diameter was plotted vs the product of the Archimedes (Ar_c) and the Prandtl number (Pr_c) of the continuous phase. If the product $Ar_c \cdot Pr_c$ exceeds 10^6 it was possible to approximate the measured results by a straight line with the slope 1/3. The particle diameter then cancels. According to refs. [7–9] the maximum heat transfer coefficient amounts to

$$\alpha_{max} = 0.12 \sqrt{\left(\frac{g^2}{\nu_c}\right)^{1/6}} \sqrt{\left(\frac{\Delta\rho}{\rho_c}\right)} \sqrt{(\lambda_c \rho_c c_c)}, \quad (4)$$

$$Pr_c = \frac{\nu_c}{a_c} > 1, \quad \frac{v_d}{w_e} > 0.1$$

where w_E is the terminal velocity of a fluid particle with a maximum stable size. The maximum depends on the physical properties of the continuous phase. The dispersed phase influences the heat transfer only by its density. Equation (4) can be used for the design of heat transfer equipment of liquid–liquid spray columns in the case when the operating conditions are near the flooding point. Experimental data of this work [10] can be described by equation (4) with an accuracy of about $\pm 40\%$. Taking into account that there are uncertainties to determine the exact flooding point and considering the few data which are available, equation (4) for the calculation of maximum heat transfer coefficients is useful. This equation does not take into account the influence of the drop diameter and the superficial velocity of the dispersed phase. Nevertheless these parameters are important as shown in Figs. 4–7. In the following section a simple heat transfer model is presented. This model takes into account that the two influencing parameters, the relative velocity w_{rel} and the average distance between the rising drops, vary with the superficial velocity. The influence of the drop diameter affecting the terminal velocity will be considered too.

HEAT TRANSFER MODEL

In a liquid–liquid spray column a swarm of drops rises to the top and induces intensive motion and mixing of the continuous phase. Hence temperature gradients in the bulk of the system are not observed. As mentioned above the temperature boundary layer is small in comparison to the drop diameter.

The heat transfer process is mainly controlled by fluid dynamics close to the heat transfer surface. In the case of gas fluidized beds the solid particles touch the heat transfer surface due to the low density ratio ρ_c/ρ_d. In a bubble or spray column the heat transfer area is covered by the continuous liquid phase. The density ratio ρ_c/ρ_d in bubble columns or gas fluidized beds is much higher than in liquid fluidized beds or spray columns [8]. Till now there have been no experimental investigations about the structure of such layers but it can be assumed that these layers in bubbles and spray columns are nearly free of fluid particles.

The continuous phase layer is locally disturbed by a drop rising in the vicinity of the surface. A drop approaching the surface displaces the continuous phase and reduces it to a thin film which remains on the surface. When the drop has passed this layer thickens again. As a result the flow of the continuous phase in this layer depends on the velocity and frequency of the drops. The relative velocity w_{rel} is assumed to be an appropriate velocity characterizing the fluid dynamics caused by the rising drops. Considering the swarm of drops the distance h between the drops depends on the volume fraction ε_d and on the drop diameter d_p and is given as

$$h = \left(\frac{\pi}{6\varepsilon_d}\right)^{1/3} d_p. \quad (5)$$

As the drop distance h decreases the continuous phase layer is more frequently disturbed and the heat transfer is improved. Increasing distance h causes the layer to grow to a large thickness, and heat transfer gets worse. Due to this effect the heat transfer process should be influenced by a characteristic length depending on the drop distance h. It was found that a modified hydraulic diameter, here called equivalent diameter D^* [equation (6)]

$$D^* = d_h \frac{d_p}{h} = \left(\frac{16\varepsilon_c^3}{9\pi\varepsilon_d^2}\right)^{1/3} d_p \quad (6)$$

is an appropriate length to describe experimental data by groups of dimensionless numbers. Kast *et al.* [11] developed this equivalent diameter to condense experimental heat and mass transfer data in packed beds.

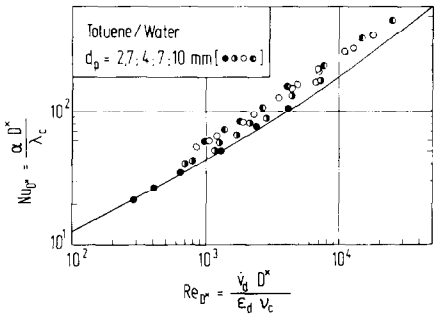

FIG. 10. Nusselt number vs Reynolds number, toluene–water system with different drop diameters.

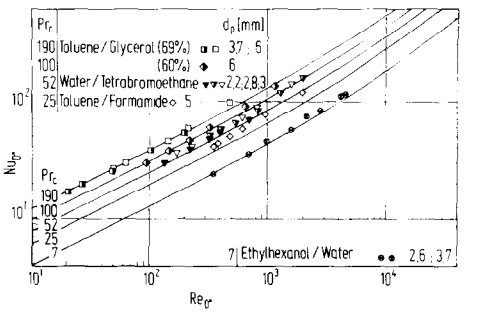

FIG. 12. Nusselt number vs Reynolds number, Pr_c = 7, 25, 52, 100, 190.

MODEL APPLIED

Experimental data obtained in the present investigation now will be described by dimensionless numbers. It is convenient to plot a Nusselt number vs a Reynolds number with the Prandtl number as a parameter. The Reynolds number is formed with the relative velocity w_{rel}, the kinematic viscosity ν_c and the equivalent diameter D^*. The Nusselt number contains the experimental heat transfer coefficient α, the equivalent diameter D^* and the thermal conductivity λ_c of the continuous phase. As an example the experimental toluene–water data obtained in the present investigation are plotted in Fig. 10. A certain influence of the drop diameter on the Nusselt number is observed. The curve shows the well-known correlation of the heat transfer on a flat plate proposed by Gnielinski [12] for use in the transition range $10^3 < Re < 10^5$: ($Re = wl/\nu_c$)

$$Nu_l = \sqrt{(Nu_{l,\text{lam}}^2 + Nu_{l,\text{turb}}^2)} \tag{6}$$

with

$$Nu_{l,\text{lam}} = 0.664 Re^{1/2} Pr^{1/3}, \quad Re_l < 10^3 \tag{7}$$

$$Nu_{l,\text{turb}} = \frac{0.037 Re_l^{0.81} Pr}{1 + 2.443 Re_l^{-0.1} (Pr^{2/3} - 1)}, \quad Re_l > 10^3. \tag{8}$$

Subscript l indicates that the dimensionless numbers are formed with the length l of the plate. The Reynolds number in equations (7) and (8) is formed with the superficial free flow velocity. Measured data obtained with the smallest drop diameter, $d_p = 2.7$ mm, correspond well to the curve calculated by equation (6) with $Pr_c = 7$. Experimental Nusselt numbers of water–tetrachloroethylene (see Fig. 11) and water–tetrabromoethane (see Fig. 12) show similar behaviour. The experimental data deviate from the calculated curves with increasing drop diameter.

Data of both toluene–glycerol systems are in good agreement with equation (6), see Fig. 12.

Discussing the heat transfer model it was assumed that the relative velocity w_{rel} characterizes the fluid dynamics in the vicinity of the heat transfer surface. The relative velocity depends on the terminal velocity w_s of single rising drops. In contrast to solid particles the terminal velocity of which increases steadily with increasing diameter, the terminal velocity of a fluid particle reaches a maximum as a certain diameter is exceeded. An oscillating drop dissipates a part of the available potential energy by the pulsing motion of the drop surface. Hence such a drop rises slower than a solid sphere with comparable physical properties because of the increased drag coefficient of the drop compared with non-pulsing solid particles. The disposable energy is dissipated by the rising velocity. Assuming that the dissipated energy of rising particles affects the heat transfer rate, the relative velocity of rising drops cannot be the only appropriate quantity in describing heat transfer. Figure 13 shows the plot of dimensionless terminal velocity of solid spheres in

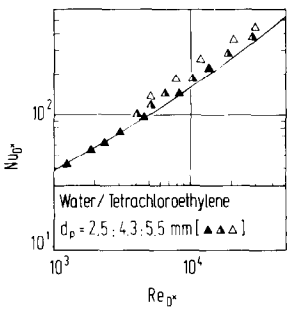

FIG. 11. Nusselt number vs Reynolds number, water–tetrachloroethylene, Pr_c = 5.

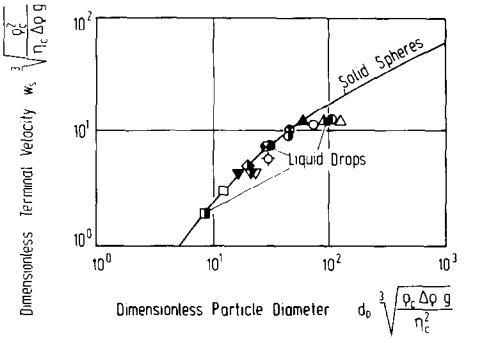

FIG. 13. Dimensionless terminal velocity of solid spheres and drops vs dimensionless particle diameter.

comparison with our own measurements of rising drops (symbols) depending on the dimensionless particle diameter. There exists a relationship between the experimental data for heat transfer represented by symbols in Figs. 10–12 and the dimensionless terminal velocity of Fig. 13. The data in Fig. 13 agree also with the curves (e.g. 2.7 mm drops in water, 2.5 mm water drops in tetrachloroethylene, etc.) in Figs. 10 and 11. Measured data, which deviate from calculated curves in Figs. 10–12 (e.g. 7 mm toluene drops in water, 5.5 mm water drops in tetrachloroethylene, 3 mm water drops in tetrabromoethane) and have a tendency to higher Nusselt numbers exhibit lower velocities in comparison with the curve of solid spheres, see Fig. 13.

The terminal velocity of solid spheres comprises the whole energy of motion available to improve the heat transfer rate. Hence a correct term

$$\frac{w_{s,\,\text{solid sphere}}}{w_{s,\,\text{liquid drop}}}$$

was introduced to enlarge the Reynolds number. The effect of this term disappears in the case of small rigid fluid particles, e.g. $d_p < 2.5$ mm toluene drops in water. On the other hand Fig. 13 shows that the corrected term can amount to 1.3, observed by out own experiments with water drops in tetrachloroethylene. This factor may explain the insufficient accuracy of equation (4) which does not take into account the diameter and the shape oscillations of drops. Experimental Nusselt numbers vs the corrected Reynolds number Re_{corr} are shown in Fig. 14 for all liquid–liquid systems.

It can be seen from this figure that a good correlation exists between experimental Nusselt numbers plotted vs the corrected Reynolds number with the curves calculated by equation (6).

WETTING PHENOMENA

All experimental data presented above were obtained with heat transfer surfaces completely covered with the continuous phase of liquid–liquid systems. Drops rising in the continuous phase may touch the heat transfer surface but do not adhere to the surface. For example this behaviour is caused by the hydrophilic property of the copper surface in the

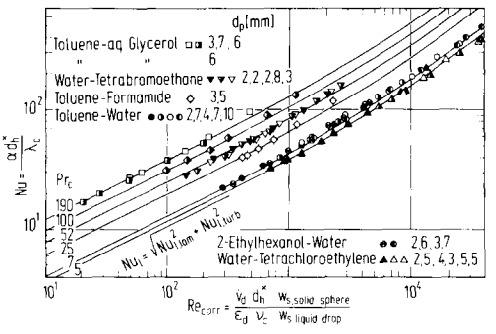

FIG. 14. Nusselt number vs corrected Reynolds number. Parameter: Prandtl number of the continuous phase.

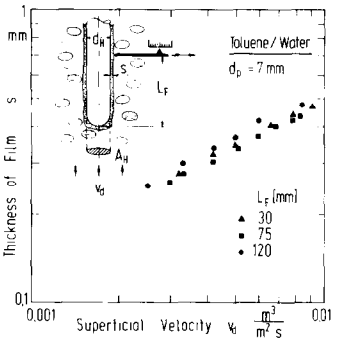

FIG. 15. Film thickness on a vertical heat transfer surface vs the superficial velocity. Parameter, length of the film L_F.

toluene–water system. Another situation can be achieved if a hydrophobic FEP surface is used in the same toluene–water system. (FEP is a fluorinated hydrocarbon with a chemical structure similar to PTFE.) In this case toluene drops, which touch the surface form a thin film covering the whole surface of the probe. This film creeps up along the surface. The total heat transfer coefficient denoted α_{tot} between the FEP-surface and the dispersion will then be influenced additionally by the thickness s of the film and by the physical properties of the dispersed phase. It is assumed that the total heat transfer resistance $1/\alpha_{tot}$ is composed of two resistances according to

$$\frac{1}{\alpha_{tot}} = \frac{1}{\alpha_d} + \frac{1}{\alpha_{d,\,dis}} \tag{9}$$

α_d denotes the heat transfer coefficient of the film formed by the dispersed phase. $\alpha_{d,\,dis}$ describes the heat transfer coefficient between the film and the liquid–liquid dispersion.

To evaluate the heat transfer coefficient α_d the film thickness s on a vertical surface was determined experimentally by an electrical conductivity probe attached to a micrometer. There is a considerable difference in the electrical conductivity of water and toluene or other organic liquids. When the tip of the probe reaches the organic film a step of electrical conductivity is observed. The film thickness s was measured at various superficial velocities $\dot{v}_d$. Figure 15 shows experimental data observed at three different vertical positions. The film thickness is constant along the surface and increases as the superficial velocity $\dot{v}_d$ rises. It is assumed that the film is formed only by drops, which rise below the vertical projection of the cross-section area A_h of the heat transfer device.

The film flow rate $\dot{V}_d$ can be estimated as

$$\dot{V}_d = \dot{v}_d \cdot A_h. \tag{10}$$

Subscript d is used to indicate that the film is formed by the dispersed phase.

The Reynolds number of the film flow is defined as

$$Re_d = \frac{\dot{m}_d}{\eta_d u} = \frac{\dot{V}_d \cdot \rho_d}{\eta_d \cdot u} \tag{11}$$

where u is the perimeter of the heater.

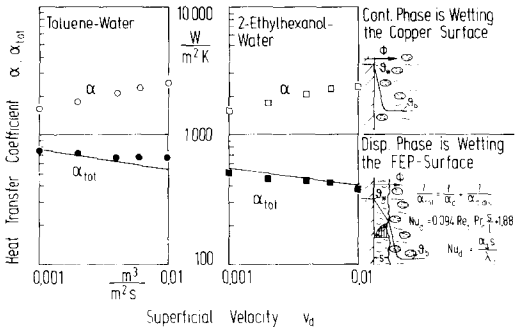

FIG. 16. Comparison between experimental and calculated data of the total heat transfer coefficient between the surface and the dispersion, toluene–water (left), 2-ethylhexanol–water (right).

Using Nusselt's equation [13]

$$Nu_l = 0.0942 Re_l Pr \frac{s}{l} \qquad (12)$$

valid for short films, the heat transfer coefficient α_d can be calculated. (The characteristic length l is equivalent to L_F.) The total heat transfer coefficient α_{tot} is obtained by equations (9) and (12) with the assumption $\alpha_{d,dis} = \alpha$. Figure 16 shows experimental data of α_{tot} in comparison with calculated values for toluene–water and 2-ethylhexanol–water. The heat transfer decreases with increasing superficial velocity. Experimental data can be correlated well by this method. Heat transfer coefficients α obtained for heat transfer areas without a covering film of dispersed phase are plotted in the upper diagram. Figure 16 demonstrates the excessive influence of thin films covering heat transfer surfaces in liquid–liquid spray columns.

REFERENCES

1. H. Kölbel, W. Siemes, R. Maas and K. Müller, Wärmeübergang an Blasensäulen, *Chemie-Ingr-Tech.* **30,** 400–404 (1958).
2. W. Kast, Analyse des Wärmeübergangs in Blasensäulen, *Int. J. Heat Mass Transfer* **5,** 329–336 (1962).
3. E. Wicke and F. Fetting, Wärmeübergang in Gaswirbelschichten, *Chemie-Ingr-Tech.* **26,** 301–309 (1954).
4. R. Wunder, Wärmeübergang an vertikalen Wärmetauscherflächen in Gaswirbelschichten, Thesis, Technische Universität München (1980).
5. A. Mersmann, Zum Flutpunkt in Flüssig/Flüssig-Gegenstromkolonnen, *Chemie-Ingr-Tech.* **52,** 933–942 (1980).
6. R. Clift, J. R. Grace and M. E. Weber, *Bubbles, Drops and Particles.* Academic Press, New York (1978).
7. A. Mersmann, Zum Wärmeübergang zwischen dispersen Zweiphasensystemen und senkrechten Heizflächen im Erdschwerefeld, *Verfahrenstechnik* **10,** 641–645 (1976).
8. A. Mersmann and R. Wunder, Preprints of the International Meeting on Heat and Mass Transfer, Toronto, Canada (1978).
9. A. Mersmann, H. Noth, D. Ringer and R. Wunder, Maximum heat transfer in equipment with dispersed two-phase systems, *Int. Chem. Engng* **22,** 16–29 (1982).
10. H. Noth, Wärmeübergang an senkrechten Wärmeübertragungsflächen in Tropfensäulen, Thesis, Technische Universität München (1982).
11. W. Kast, O. Krischer, H. Reinicke and K. Wintermantel, *Konvektiver Wärme- und Stoffübergang.* Springer, Berlin (1974).
12. V. Gnielinski, Berechnung mittlerer Wärme- und Stoffübergangskoeffizienten an laminar und turbulent überströmte Einzelkörper mit Hilfe einer einheitlichen Gleichung, *Forsch. Geb. Ing Wes.* **41** (1975).
13. W. Nusselt, Die Oberflächenkondensation des Wasserdampfes, *Z. Ver. Dt. Ing.* **60,** 541–546 (1916).

PHENOMENES DE TRANSFERT THERMIQUE DANS DES COLONNES DE BROUILLARD LIQUIDE–LIQUIDE

Résumé—Des expériences de transfert thermique concernent des surfaces cylindriques immergées dans des colonnes de brouillard liquide-liquide de 100 et 200 mm de diamètre. On utilise eau, formamide, glycerol, tetrachloréthylène, tétrabromoethane, toluène et 2-éthylhexanol pour étudier, dans un large domaine, l'influence des propriétés physiques des liquides non miscibles. Les conditions opératoires (débit du liquide de la phase dispersée, géométrie de l'équipement) affectent faiblement le transfert thermique. Les propriétés physiques de la surface chauffante sont variées pour examiner l'influence des phénomènes de mouillage sur le coefficient de transfert thermique. Ce modèle de calcul présenté ici est basé sur des équations de transfert thermique dans un écoulement monophasique sur plaque plane. Le transfert thermique est décrit par un nombre de Reynolds incorporant la vitesse relative entre les gouttes et la phase continue, le diamètre équivalent et la viscosité de la phase continue.

WÄRMEÜBERGANG IN TROPFENSÄULEN

Zusammenfassung—Messungen zum Wärmeübergang zwischen einem zylindrischen Heiz-element und einer Flüssig-Flüssig-Dispersion wurden an Kolonnen mit 100 und 200 mm Durchmesser durchgeführt. Als Flüssigkeiten kamen Wasser, Formamid, Glyzerin, Tetrachloräthylen, Tetrabromethan, Toluol und 2-Äthylhexanol zum Einsatz, um den Einfluß der physikalischen Eigenschaften von nichtmischbaren Flüssigkeiten in einem weiten Bereich zu variieren. Betriebsbedingungen, wie z.B. die Volumendichte der dispersen Phase und auch die Geometrie der Kolonne beeinflussen den Wärmeübergang relativ wenig. Die physikalischen Eigenschaften der Heizfläche wurden variiert, um den Einfluß von Benetzungsphänomenen auf den Wärmeübergang zu untersuchen. Die Berechnungsmethode dieses Aufsatzes stützt sich auf Wärmeübergangsgleichungen für die einphasige Strömung über eine Platte.

ЯВЛЕНИЯ ТЕПЛОПЕРЕНОСА В ЖИДКОСТЬ-ЖИДКОСТНЫХ КОЛОНКАХ РАСПЫЛА

Аннотация—Экспериментально исследовался теплоперенос от цилиндрических поверхностей, находящихся в жидкость-жидкостных колонках распыла диаметром 100 и 200 мм. Для исследования влияния в широком диапазоне физических свойств несмешивающихся жидкостей использовались вода, формамид, глицерин, тетрахлорэтилен, тетрабромэтан, толуэн, 2-этилгексанол. Рабочие параметры (скорость течения жидкости в дисперсной фазе, геометрия установки) оказывают слабое влияние на процесс теплопереноса. Для исследования влияния явления смачивания на коэффициент теплопереноса использовались поверхности с различными физическими свойствами. Представленная в работе расчетная модель основана на уравнениях теплопереноса для обтекания плоской пластины однофазным потоком жидкости. Теплоперенос описывается числом Рейнольдса, включающим относительную скорость капель и сплошной фазы, эффективный диаметр и вязкость сплошной фазы.